The structural determination and skeletal ring modes of tetrahydropyran

Sébastien Gruet, Olivier Pirali, Amanda Steber, Melanie Schnell

Journal Name

ARTICLE TYPE

Cite this: DOI: 10.1039/xxxxxxxxxx

The structural determination and skeletal ring modes of tetrahydropyran†

Sébastien Gruet,*[a,b,c,d,‡] Olivier Pirali,[e,f] Amanda L. Steber,[a,b,c,d] and Melanie Schnell*[a,b,c,d]

Received Date
Accepted Date

DOI: 10.1039/xxxxxxxxxx

www.rsc.org/journalname

A high-resolution molecular spectroscopy study was carried out on the cyclic ether tetrahydropyran (THP), one of the smallest molecules composed of a pyranose ring. As this ring structure is closely related to carbohydrates, THP can offer relevant insight into structural variations of this unit. Thus, an extensive probe of THP using three broadband instruments ranging from the microwave to the far-infrared (2-8 GHz, 75-110 GHz and 100-650 cm^{-1} frequency ranges) was performed to accrue both accurate sets of rotational constants and structural information. This array of experimental setups provided an accurate set of data to improve the description of the ground state of THP and revise the principal parameters of its backbone structure. In addition, the complementary dataset obtained from these experiments led to a better characterization of the vibrational motions involving the skeletal ring of the molecule. In particular, the vibrational frequencies of four of these modes (ν_{23} (∼250 cm^{-1}), ν_{22} (∼403 cm^{-1}), ν_{21} (∼430 cm^{-1}), and ν_{20} (∼562 cm^{-1})) have been determined from the analysis of the first rotationally resolved vibrational spectrum reported for THP. Quantum-chemical calculations aided in the analysis of the experimental results.

1 Introduction

Tetrahydropyran (THP), also known as pentamethylene oxide or oxane, is a non-aromatic six-membered heterocyclic compound. As a cyclic ether, it possesses a ring backbone structure characteristic of the pyranose family, in which all members consist of a ring containing five carbon atoms and one oxygen atom. This defining pyranose ring is the core structure of biomolecules belonging to the carbohydrate molecular family, such as the monosaccharides glucose and ribose. Carbohydrates are involved in numerous important mechanisms in living organisms. For example, ribose is one of the backbone molecules of the nucleic acid RNA, which is essential in gene formation processes. Furthermore, ribose derivatives, like deoxyribose and adenosine triphosphate (ATP), are also key players in biology. Deoxyribose is a sugar component of DNA, and ATP plays a central role in metabolic reactions as an energy-storage molecule, which underlines the biological relevance of such structural units.

The spectroscopic investigations of cyclic ethers in the gas phase have been mostly centered on the exploration of the conformational landscape.[1–4] Important contributions come from microwave spectroscopic studies, in which many of the conformeric properties were determined.[4] Infrared spectroscopy was also used to identify the low frequency vibrational modes of these molecules.[5,6] The ring puckering modes observed in the far-infrared frequency range are of particular interest as the vibrational frequencies are strongly dependent on the molecular conformation.

The pure rotational spectrum of the THP vibronic ground state was investigated more than 40 years ago by Rao and Kewley[7] and Lowe and Kewley[8] between 8 and 40 GHz, and the dipole moment was experimentally determined. The ^{13}C isotopologues of THP were observed in a study reported by Spoerel *et al.*[9] which targeted the THP-water complex using molecular-beam Fourier-transform microwave spectroscopy (3-26.5 GHz). This study provided partial information on the molecular structure of THP. In

[a] *Deutsches Elektronen-Synchrotron, Notkestraße 85, D-22607 Hamburg, Germany; E-mail: melanie.schnell@desy.de*
[b] *The Hamburg Centre for Ultrafast Imaging, Luruper Chaussee 149, D-22761 Hamburg, Germany*
[c] *Institut für Physikalische Chemie, Christian-Albrechts-Universität zu Kiel, Max-Eyth-Straße 1, D-24118 Kiel, Germany*
[d] *Max-Planck-Institut für Struktur und Dynamik der Materie, Luruper Chaussee 149, D-22761 Hamburg, Germany*
[e] *AILES beamline, Synchrotron SOLEIL, L'Orme des Merisiers, Saint Aubin BP 48, F-91192 Gif sur Yvette Cedex, France*
[f] *Institut des Sciences Moléculaires d'Orsay, UMR 8214 CNRS, Université Paris-Saclay, F-91405 Orsay, France*
† Electronic Supplementary Information (ESI) available: [details of any supplementary information available should be included here]. See DOI: 10.1039/b000000x/
‡ Present adress: Univ. Lille, CNRS, UMR 8523, Physique des Lasers, Atomes et Molécules, F-59000 Lille, France; sebastien.gruet@univ-lille.fr

the infrared, data in the gas phase are limited to the work of Vedal *et al.* [10] (1975), who recorded and assigned the low resolution spectrum of THP in the 200-4000 cm^{-1} region. In 1986, Lopez *et al.* [11] reported the observation of six vibrationally excited states by microwave spectroscopy (18-40 GHz).

In this paper, we report an extensive study of THP at high resolution from the microwave to the far-infrared domain. The first rotationally resolved vibrational spectrum of THP is provided along with the analysis of four fundamental rovibrational bands. The ground state of the molecule is reinvestigated, and we also report the comprehensive study of several vibrational satellites of THP by pure rotational spectroscopy. This includes the six skeletal ring motions of the molecule. The vibrationally excited states were assigned accordingly with the IR analysis and supported by density functional theory (DFT) anharmonic calculations. The sensitivity of our microwave and millimeter wave spectroscopy experiments allowed us to determine a very accurate set of data for the ^{13}C and ^{18}O isotopologues in order to revisit the backbone structure of THP. The accurate measurements of their frequencies might be good checkpoints to test the quality of quantum-chemical calculations.

2 Experimental details

During this study, three broadband apparatus were used to cover the spectral ranges from 2-8 GHz, 75-110 GHz and 50-650 cm^{-1}. An overview of all the experimental techniques is discussed in some detail below, and the three recorded spectra are shown in Figure 1. These complementary techniques led to the observation and the analysis of the ground vibrational state and seven vibrationally excited states of THP. The sample was purchased from Sigma Aldrich (99 % pure), and it was used at room temperature (298 K) without further purification.

2.1 Microwave region

The pure rotational spectrum of THP was recorded from 2 to 8 GHz using the chirped pulse Fourier transform microwave (CP-FTMW) [12,13] spectrometer COMPACT. The spectrometer configuration has been described in more detail elsewhere. [14,15] A General Valve pulse nozzle (Parker) delivers the molecular beam perpendicular to the microwave pulse propagating between two horn antennas. A pulse duration of 4 μs was used, and the free induction decays (FIDs) were collected for 40 μs. Approximately 3 bar of neon was used as the backing gas for the supersonic expansion, which resulted in an approximate molecular rotational temperature of 2 K. The signal-to-noise ratio of about 2000:1 obtained for the ground state after 500000 FID averages was sufficient to observe the ^{13}C and the ^{18}O isotopologues of THP in natural abundance. Note that nine rotational transitions involving the lowest lying vibrational state ν_{42} ($F_{calc} = 238.4$ cm^{-1}) of THP were also present in the jet-cooled spectrum.

2.2 Millimeter wave region

In addition to the data between 2 and 8 GHz, the pure rotational spectrum of THP was extended to the millimeter wave region with a commercial segmented chirped pulse Fourier-transform millimeter wave spectrometer (CP-FTMMW, also referenced as Fourier-transform Molecular Rotational Resonance spectrometer, FT-MRR) purchased from Brightspec. It operates over 75-110 GHz (W-band). Information about the segmented chirped pulse technique can be found in Neill *et al.* [16], and technical details concerning the spectrometer have been described in recent publications. [17,18] The spectrometer is coupled with a 67 cm long stainless-steel single pass cell, which is sealed with two Teflon windows at each side. A flow of about 6 μbar of THP was maintained inside the chamber at room temperature during the experiment. The molecular response covering 75-110 GHz in the form of an FID was collected by a receiving horn antenna. In the high dynamic range mode, the excitation pulse duration was 250 ns, and each FID was collected for 4 μs. A total of 4.5 million spectral acquisitions were recorded and averaged. This corresponds to a measurement time of about 9 hours.

2.3 Far-infrared domain

The rotationally resolved absorption spectrum in the far-infrared domain of THP was investigated with the AILES (Advanced Infrared Line Exploited for Spectroscopy) beamline at the synchrotron facility SOLEIL. The rotational-vibrational spectrum was recorded with a Fourier-transform infrared spectrometer (Bruker IFS 125) using the far-infrared emission of the synchrotron radiation as a continuum source. [19] The 50-650 cm^{-1} spectral range was obtained with a 6 μm Mylar beamsplitter and a 4 K Si-bolometer detector. A reservoir of THP was connected to a long optical path length cell (150 m) in a "White" type optical arrangement, and 50 μbar of vapor pressure was injected at room temperature into the cell. Using the maximum resolution of the instrument (0.001 cm^{-1}) was mandatory to resolve the very dense rotational structure of each vibrational band observed. A 1.5 mm diameter iris was used in order to maintain this resolution over the entire spectral range of interest. The final spectrum is an average of 400 scans corresponding to an acquisition time of about 24 hours.

3 Results & Discussions

THP is a near oblate asymmetric molecule ($\kappa = 0.83$), existing predominantly in a chair configuration at room temperature. [20] The permanent electric dipole moment of the molecule is along the *a* inertial axis ($\mu_a = 1.39$ *D*) and, with a smaller contribution, along the *c*-axis ($\mu_c = 0.74$ *D*). [7] The pure rotational spectrum of each vibrational state in the millimeter wave region is characterized by intense, relatively isolated transitions (*a*-type) and a large series of *c*-type transitions spaced by ~4 GHz (see Figure 1(b)). In the far-infrared region, all of the modes exhibit an A/C shape band contour recognizable by a sharp, predominant *Q* branch when compared to the *P* and *R* branches. The spectra in the millimeter wave and the far-infrared domains have been recorded at room temperature and contain a high density of lines complicating the analysis. The assignment in the microwave and in the millimeter wave regions were performed using the AABS package [21], while in the far-infrared the Loomis Wood diagrams [22] employing the ground state combination difference (GSCD) tech-

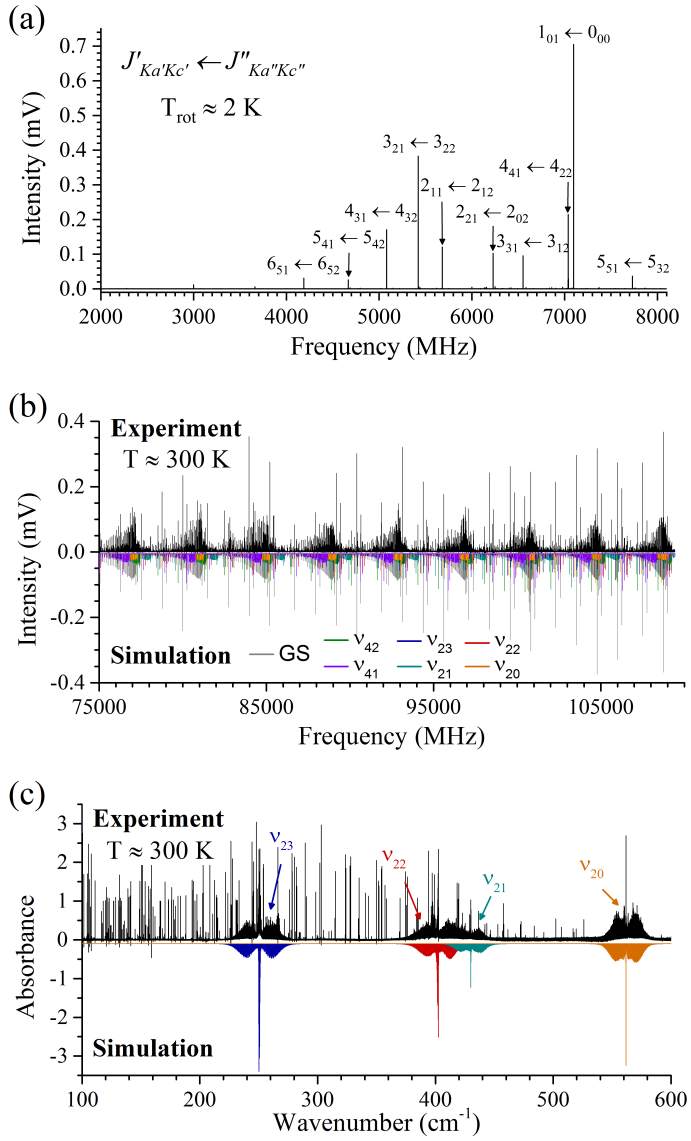

Fig. 1 Overview of the experimental spectra. (a) Spectrum recorded with the CP-FTMW spectrometer COMPACT between 2-8 GHz. The intense transitions of the THP ground state are assigned. (b) Spectrum recorded with the CP-FTMMW spectrometer between 75-110 GHz at room temperature (black trace). The ground state and six fundamental vibrationally excited state (lowest in energy) spectra are simulated below the experimental spectrum. The simulated spectra were derived from the results of our fits (see text). (c) Broadband spectrum recorded in the far-infrared (100-650 cm^{-1}) with the FTIR spectrometer at room temperature. The upper trace is the experimental spectrum while the lower trace is a spectrum simulated from our experimental parameters. The four vibrational bands are located at about 250 cm^{-1} (ν_{23}), 402 cm^{-1} (ν_{22}), 430 cm^{-1} (ν_{21}) and 562 cm^{-1} (ν_{20}). The sharp lines all across the spectrum are intense transitions of water present as an impurity.

nique was required to identify and assign the rovibrational transitions. The density of lines in the vibrational bands observed in the far-infrared spectrum is so high that most of the lines are blended. The GSCD technique is a reliable method to unambiguously assign transitions in such congested spectra. The assignment was supported by density functional theory (DFT) anharmonic calculations performed at the B3LYP/cc-pVTZ level of theory using Gaussian09[23]. All data have been fit with the SPFIT/SPCAT program[24] suite using an effective Hamiltonian (Watson's A reduction) in a III^l representation. Line lists of the transitions used for each fit are available in the supplementary materials.†

3.1 Ground state and isotopologues

The study of the THP ground state by Lowe and Kewley[8] in 1976 reported an analysis covering low values of J and K_a in the 8-40 GHz spectral range, and it was never extended to higher frequency. Note that Lopez *et al.*[11] did provide a new set of rotational constants in 1986, but they were determined using the same dataset from Lowe and Kewley[8] with a modern Hamiltonian. The precision of the ground state rotational energy levels is a critical parameter for interpreting the rovibrational spectrum that we recorded in the far-infrared. Indeed, the IR analysis is based on the use of the GSCD, which relies on the accuracy of the lower state. A global fit, including 665 transitions measured in this work at higher resolution and higher frequency and the original dataset from Lowe and Kewley[8], significantly improved the ground state fit of THP. These new transitions involve a wider range of quantum numbers up to J = 93 and K_a = 67. The result of the combined fit, which includes data from the 2-8 and 75-110 GHz frequency ranges, is summarized in Table 1.

Table 1 Rotational constants of the ground state of THP. Uncertainties on the last digits are indicated in parentheses. Our fit includes data from the 2-8 and 75-110 GHz frequency ranges

Parameters	Theory*	Lowe and Kewley[8]	Our Work	Our Work + ref[8]
A [MHz]	4610.718	4673.5022(88)	4673.50790(26)	4673.50798(26)
B [MHz]	4458.993	4495.0739(88)	4495.07734(24)	4495.07731(24)
C [MHz]	2563.136	2601.2802(91)	2601.28065(35)	2601.28056(34)
Δ_J [kHz]	1.0729	1.03(21)	1.08514(60)	1.08521(60)
Δ_{JK} [kHz]	-1.7227	-1.7710(82)	-1.7723(12)	-1.7729(11)
Δ_K [kHz]	0.8406	0.947(43)	0.88097(85)	0.88135(83)
δ_J [kHz]	0.0150	0.01454(90)	0.012376(85)	0.012330(82)
δ_K [kHz]	1.6510	1.685(32)	1.6320(81)	1.6361(78)
Φ_{JK} [Hz]	-0.00110	-	-0.003234(14)	-0.003230(13)
Φ_{KJ} [Hz]	0.00662	-	0.00704(12)	0.00699(12)
rms [kHz]		118	26.9	50.3
# of lines		65	665	730
J		1-32	0-93	0-93
K_a		0-23	0-67	0-67

*B3LYP/cc-pVTZ

In addition to the ground state transitions for the main isotopologue, the high dynamic range of our spectra (2000:1) allowed for the assignment of all the singly substituted ^{13}C isotopologues of THP in natural abundance in the microwave and the millimeter wave regions. This was further supported by the fact that THP is a C_s symmetric molecule, which means that two of the carbon positions are equivalent on either side of the ring causing their transition intensity to double. Furthermore, the ^{18}O isotopologue of THP was observed in the microwave spectrum between 2 to 8 GHz (see Figure 2), which was not reported before. The nu-

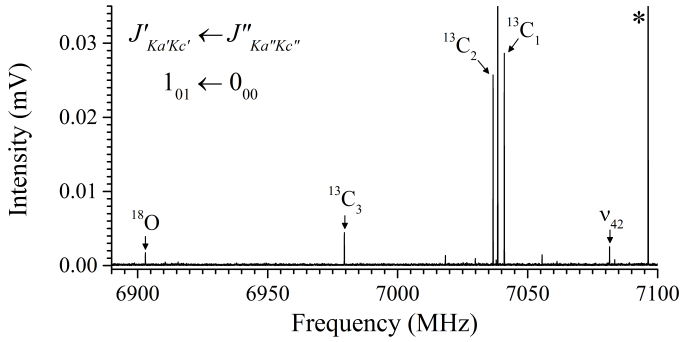

Fig. 2 Example of observed rotational transitions for the isotopologues of THP in the microwave frequency range. The transition assigned for all species represented in this spectral zoom-in corresponds to the $1_{01} \leftarrow 0_{00}$ transition. The parent transition is represented by an asterisk (*), and its intensity is cut by the vertical axis values. Note that the $^{13}C_1$ and $^{13}C_2$ transitions are more intense than the $^{13}C_3$ transition due to symmetry. In fact, the carbon atoms C_1 and C_5 are equivalent by symmetry, as C_2 and C_4.

merous lines we observed for the ^{13}C isotopologues in addition to the lines reported by Spoerel *et al.*[9] resulted in the accurate determination of the centrifugal distortion constants D_J, D_{JK}, D_K. However, due to the limited number of lines for the ^{18}O isotopologue, only the principal rotational parameters were determined. The quartic constants were fixed to the ground state values. The results of the fits can be found in the supplementary materials (Table S1).†

The data obtained from the analysis of the ^{13}C and ^{18}O isotopologues were used to determine the coordinates of the atoms which form the ring backbone of the molecule. The substitution structure (r_s) has been extracted from the Kraitchman's equations[25] implemented in the KRA program developed by Z. Kisiel[26]. The structural parameters are presented in Table 2, and the comparison between the r_s structure (experimental) and the calculated structure (B3LYP/cc-pVTZ) in Figure 3 shows a good agreement.

Table 2 Structural parameters of THP and their comparison with related molecular species. Numbering of atoms according to Figure 3

	This Work	THP Ref[9]	Cyclohexane Ref[27]	Piperidine Ref[28]	1,4-Dioxane Ref[29]	Glucose B3LYP/aVTZ
Bond						
C1-C2	1.5220(39)	1.516	1.5300(32)	1.530(1)	1.510(4)	1.53
C2-C3	1.5300(32)	1.530	1.5300(32)			1.52
CO	1.4201(34)	[1.413]	-	-	1.417(2)	1.42
Angle						
C1-C2-C3	110.16(28)	110.17	111.28(30)	111.1(7)	-	110.1
C2-C3-C4	109.63(27)	109.73	111.28(30)	109.6(13)	-	110.4
C4-C5-O	111.86(31)	[114.66]	-	-	111.1(3)	109.5
C5-O-C1	111.41(32)	[114.8]	-	-	110.9(10)	115.4
Dihedral						
C5-C4-C2-C3	132.15(64)	132.31	130.77	131.6(8)	-	129.9
C4-C5-C1-O	125.96(63)	[132.31]	-	-	129.4(7)	125.6
C3-C4-C5-X	56.50(64) (X=O)	- -	55.26(82) (X=C)	57.2(5) (X=NH)	- -	55.7 (X=O)

The values obtained for the C2-C3 bond, the C1-C2-C3 and C2-C3-C4 angles, as well as the C5-C4-C2-C3 dihedral angle (or their equivalent lengths and angles which are going to be the same by symmetry) are identical to those reported by Spoerel *et al.*[9]. These values are dependent only on atoms that are affected by the surrounding carbon atoms. However, there is a discrepancy in the value reported for the C1-C2 bond and our value, which is longer than reported before. This discrepancy primarily arises from the fact that they constrained the CO bond to 1.413 Å, which is shorter than our experimentally determined value of 1.4201(34) Å. The C1-C2 bond (1.5220(39) Å), due to the influence of the oxygen atom, is also shorter than the CC bond (sp^3 hybridization) observed for cyclohexane (1.5300(32) Å), which points to some sp^2 hybridized character. Furthermore, when we examine molecules sharing structural similarities with THP, like piperidine (the O atom is replaced by a NH group) and 1,4-dioxane (the CH_2 group opposite to the O atom is replaced by a second O atom), certain similarities to THP can be observed. As can be seen in Table 3, the C2-C3-C4 angle values of THP and piperidine are very close, as are the C4-C5-O and C5-O-C1 angle values between THP and 1,4-dioxane. These observations show that the impact of the neighboring second-order atoms for identical structural parts of these molecules is limited. The dihedral angle C3-C4-C5-O of THP is also comparable to those determined for cyclohexane and piperidine, which means that the out-of-plane angles in cyclohexane are not strongly affected by the replacement of a methylene group by an oxygen atom or a NH group. A comparison with the structure of a more complex biomolecule like glucose also indicates that the pyranose ring is relatively robust and not drastically affected by the addition of several functional groups. This robustness indicates that the pyranose ring will most likely retain its structure once it has been incorporated into a larger molecular system like a carbohydrate.

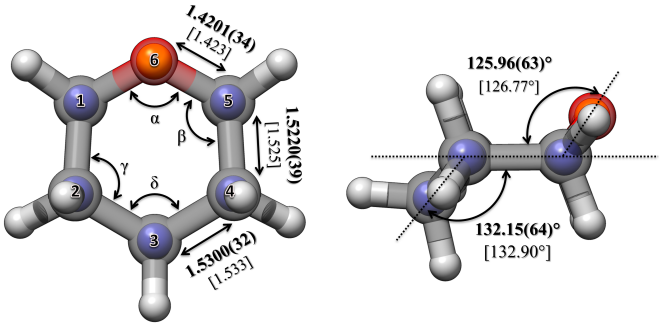

Fig. 3 Top view (left) and side view (right) of THP at the calculated equilibrium geometry (B3LYP/cc-pVTZ). The blue spheres correspond to the substitution structure determined with Kraitchman's equations (see text). The bond values are in Å. $\alpha = 111.41(32)^\circ$ [112.36°], $\beta = 111.86(31)^\circ$ [111.94°], $\gamma = 110.16(28)^\circ$ [110.40°] and $\delta = 109.63(27)^\circ$ [110.20°]. Values in square brackets are deduced from our calculations.

3.2 Excited vibrational states

3.2.1 Infrared study.

As THP is a C_s symmetric molecule, it possesses 42 fundamental vibrational modes, 23 A' symmetry and 19 A" symmetry. All of the vibrational modes are IR active, and according to our anharmonic calculations (B3LYP/cc-pVTZ), six fundamental excited states are expected to be present below 600 cm^{-1}. The six states correspond to the six skeletal motions of the molecule, and a representation of the ring deformations caused by the vibrational

motions is depicted in Figure 4. An overview of the far-infrared spectrum from 100 to 600 cm^{-1} is shown in Figure 1(c). The assignment of the four vibrational bands in the spectrum, i.e., ν_{23}, ν_{22}, ν_{21} and ν_{20} located at 250, 402, 430 and 562 cm^{-1} respectively, was relatively straight forward using the predicted frequency of each band and their calculated infrared intensities from the anharmonic calculations. The two other modes, denominated as ν_{42} ($F_{calc} = 238.4$ cm^{-1}, $I_{calc} = 0.32$ km mol^{-1}) and ν_{41} ($F_{calc} = 466.1$ cm^{-1}, $I_{calc} = 0.002$ km mol^{-1}), have calculated infrared intensities that are too weak to be observed in the spectrum. Indeed, their intensities are at least five times lower than ν_{21} ($I_{calc} = 1.71$ km mol^{-1}), which is the weakest vibrational band observed in our spectrum. However, note that it is difficult to distinguish if ν_{42} (which possesses a *b*-type band contour) is actually present in the spectrum due to its promiscuity with the intense ν_{23} vibrational band (*a*-/*c*-type hybrid band contour). These observations are in good agreement with the low resolution infrared work in the vapor phase reported by Vedal *et al.* [10].

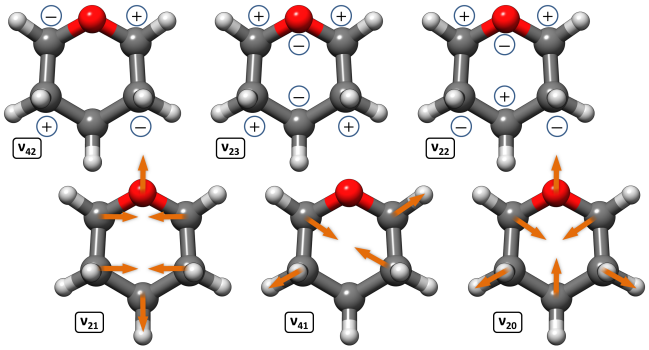

Fig. 4 Schematic view of the six skeletal modes of THP. Only the ring atom motions are represented. The positive and negative signs indicate an out-of-plane movement.

The experimental IR spectrum shows a relatively good S/N ratio, and a resolution of 0.001 cm^{-1} was sufficient to rotationally resolve the $P-$ and $R-$branches of each band. However, the $Q-$branches were only partially resolved due to the accumulation of lines and the presence of hot bands involving the low lying vibrational modes of the molecule. Calibration of the IR spectrum was performed using strong transitions of water impurities.[30,31] As mentioned previously, the high resolution infrared data were analyzed using the Loomis-Wood diagrams due to the very high density of lines of each vibrational band. The ground state parameters used to perform the GSCD were those determined from our reinvestigation of the ground state performed in the previous section. Several thousand of transitions, with an estimated accuracy of 0.0002 cm^{-1}, have been assigned for each band. $a-$ and $c-$type transitions were observed for ν_{23} and ν_{22} while only $a-$type transitions were available for ν_{21} and ν_{20}. This was due to the fact that the strengths of infrared transitions depend on the variation of the dipole moment along the vibrational motion coordinate. The large data set and the wide range of quantum numbers led to the determination of precise band centers and accurate Hamiltonian parameters for each vibrational band. For example, ν_{22} involves transitions with J values up to 67 and K_a values up to 36. The results of all the fits are presented in Table S2.†Figure 5 shows a portion of the ν_{20} experimental infrared spectrum in the *R*-branch region with the corresponding simulated spectrum obtained from the final set of parameters. It can be seen that despite the high spectral density, the frequencies of the rovibrational transitions are reproduced well. However, many relatively intense lines remain unassigned in the experimental spectrum. They belong to the numerous hot bands which are significantly populated at room temperature.

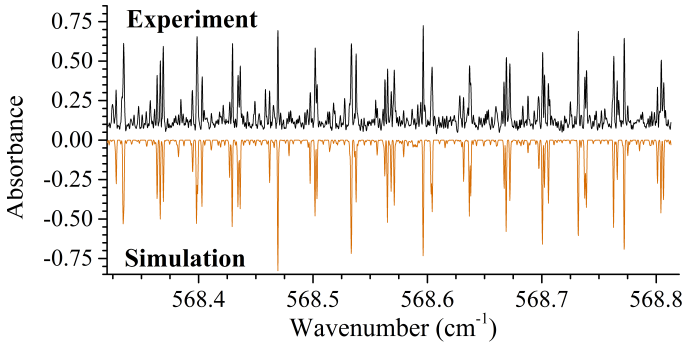

Fig. 5 Zoom-in of the ν_{20} vibrational band R-branch located at 562 cm^{-1}. The upper trace is the experimental spectrum while the lower trace is a simulated spectrum based on fitted experimental parameters.

3.2.2 Millimeter wave study.

In the 75-110 GHz spectral range, three vibrational satellites were observed in addition to the four also observed in the far-IR work, giving a total of seven states (see Figure 6). According to the anharmonic calculations, nine excited states have an energy below 600 cm^{-1}: the six fundamental modes already mentioned previously, two overtones ($2\nu_{42}$ and $2\nu_{23}$ calculated at 470 cm^{-1} and 480 cm^{-1}, respectively) and a combination band (($\nu_{42}+\nu_{23}$) calculated at 474 cm^{-1}). In the work initiated by Lopez *et al.* [11] six vibrational states were assigned in the 18-40 GHz range. In our spectrum, we successfully identified and characterized seven vibrational states but ν_{42}, ν_{23}, and ($\nu_{42}+\nu_{23}$) were found to be perturbed.

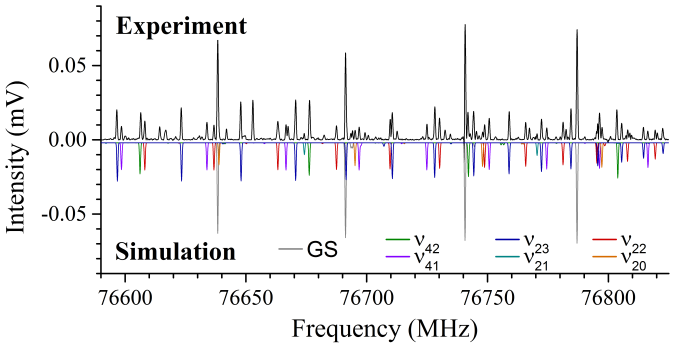

Fig. 6 Vibrational satellites of THP in the mmw region. The upper trace is the experimental spectrum while the lower traces are simulated spectra calculated from the experimental rotational constants (Table 3). A good agreement can be observed for the ground state and each vibrational excited state.

For these perturbed states, only a limited number of transi-

Table 3 Results of the fits obtained for the six fundamental excited states observed. Values in square brackets are fixed to the ground state values of THP. Uncertainties on the last digits are indicated in parentheses

Parameters	ν_{42}*	ν_{23}*	ν_{22}	ν_{21}	ν_{41}	ν_{20}
Band Center (cm^{-1})	-	250.1409355(50)	402.6817372(40)	430.0384605(53)	-	561.8969024(43)
A [MHz]	4672.0523(11)	4666.69499(71)	4663.73042(65)	4672.2381(10)	4679.8477(10)	4672.22948(26)
B [MHz]	4489.9567(11)	4494.24093(52)	4478.16085(56)	4511.00066(87)	4493.22875(97)	4493.98291(17)
C [MHz]	2591.5531(14)	2608.57532(69)	2597.87176(18)	2586.52925(17)	2611.65390(59)	2598.67716(15)
Δ_J [kHz]	1.0840(66)	1.0869(19)	0.91604(18)	1.24036(24)	1.1016(13)	1.083644(44)
Δ_{JK} [kHz]	-1.655(11)	-1.8831(68)	-1.34681(20)	-2.10418(24)	-1.83970(20)	-1.773406(87)
Δ_K [kHz]	0.4510(98)	1.2744(55)	0.62278(26)	0.84832(29)	1.15403(24)	0.88211(16)
δ_J [kHz]	0.0127(18)	0.0036(12)	-0.05784(10)	0.09253(13)	0.001726(98)	0.012743(30)
δ_K [kHz]	1.229(51)	2.491(42)	[1.6361]	[1.636113469]	[1.6361]	[1.6361]
Φ_J [Hz]	-0.0460(72)	0.0194(15)	-0.005222(40)	0.005284(55)	-	-
Φ_{JK} [Hz]	2.815(39)	-0.700(17)	0.018671(55)	-0.026862(56)	-0.000565(41)	-0.003137(22)
Φ_{KJ} [Hz]	-8.70(12)	2.049(42)	-0.02446(20)	0.04363(24)	-	0.007004(45)
Φ_K [Hz]	5.886(75)	-1.351(26)	0.01414(15)	-0.02370(16)	-	-
MW rms [kHz]	30.2	30.8	37.2	32.6	32.8	32.1
IR rms [cm^{-1}]	-	0.00014	0.00013	0.00014	-	0.00014
# of lines (MW/IR)	256	254/1780	387/3067	379/1942	387	367/2904
J (MW/IR)	0-71/-	8-79/7-53	8-71/0-67	8-74/0-49	9-76/-	8-76/3-79
Ka (MW/IR)	0-48/-	0-52/0-31	0-47/0-36	3-74/0-21	0-52/-	0-52/0-25
Band Center Harm.(Anharm.)	238.4(235.3)	243.3(239.4)	393.3(395.1)	437.5(435.6)	466.1(459.1)	566.2(567.8)
A_{calc} [MHz]	4671.38	4667.57	4664.63	4673.21	4679.32	4672.76
B_{calc} [MHz]	4490.25	4493.85	4482.61	4506.35	4493.61	4494.27
C_{calc} [MHz]	2585.72	2614.41	2597.68	2586.47	2613.18	2599.03

*Only a limited number of parameters for those perturbed states are shown in this table. Please refer to Table S3 and Table S6 in the supplementary materials for the full table.†

tions could be used for the fits while for the non-perturbed states, several hundreds of lines have been assigned and used to fit the Hamiltonian parameters. For the excited states also observed in the far-infrared domain, combined fits were performed including the millimeter wave and infrared data. Table 3 summarizes the rotational constants for the six fundamental excited states. The results of the fits including only the millimeter-wave data are also provided in the supplementary materials (Table S3)†, and a zoom-in of the mmw spectrum is presented in Figure 6 to show the good agreement between the simulation performed with the determined rotational constants and the experimental spectrum.

From our analysis in the far-infrared frequency range, four vibrational states were assigned unambiguously, and three additional states were identified by comparison with our anharmonic calculations. The two last states lying below 600 cm^{-1} in energy, $2\nu_{42}$ and $2\nu_{23}$, were not observed, but we believe that they might be strongly perturbed as they are close in energy not only to each other but also with $(\nu_{42}+\nu_{23})$.

Note that despite the assignment of the ν_{23} in the far-infrared region without any particular difficulty, we observed strong perturbations when assigning its pure rotational spectrum. A similar case was observed with the two lowest vibrational states of quinoline.[32] The main reason for this was simply the lower resolution of the FTIR spectrometer compared to the technique used in the millimeter wave range. This lower resolution made it so that there was no noticeable perturbation on the transitions in the FTIR spectrum. For THP, ν_{23} and ν_{42} were thought to be involved in Coriolis coupling as the difference in energy between those two states is less than 5 cm^{-1} according to our anharmonic calculations. Concerning the energy order of ν_{42} and ν_{23}, we assume that ν_{42} is the excited state with the lowest energy because weak transitions of ν_{42} were observed in our spectrum recorded by jet-cooled rotational spectroscopy in the 2-8 GHz range (*vide supra*). We have not been able to account for this perturbation even with the implementation of Coriolis interaction terms into the Hamiltonian, and thus only a partial fit was successful.

The comparison with the work of Lopez *et al.*[11] shows a good agreement with our results. The higher frequency range of our experiment allowed us to accurately determine the quartic centrifugal distortions constants, which were not previously well determined. The accurate parameters for each state from our CP-FTMMW experiment were valuable input during the process of analyzing the infrared data.

4 Conclusions & Outlook

The ground state of THP has been reinvestigated to improve the spectroscopic parameters. This was key in the rovibrational analysis in the IR range using the GSCD technique. The first observation of the ^{18}O isotopologue in natural abundance combined with the ^{13}C isotopologue data led to the complete characterization of the ring backbone structure of the molecule, and the experimental substitution structure determined from this analysis reveals the impact of the replacement of a methylene group by an oxygen atom in the structure of cyclohexane. In particular, the CC bonds neighboring the oxygen atom become shorter (1.5220(39) Å) compared to the other CC bonds in THP or in cyclohexane (1.5300(32) Å).

Aside from the ground vibrational state, seven excited vibrational states occurring below 600 cm^{-1} in energy were observed in the millimeter range. Four of them were assigned unambigu-

ously thanks to the rovibrational analysis performed in the far-infrared frequency range, leading to an accurate determination of their band centers. The identification of the three remaining states was supported by our anharmonic calculations. ν_{42}, ν_{23}, and $(\nu_{42}+\nu_{23})$ were found to exhibit transitions with relatively strong perturbations that could not be solved considering the narrow spectral range in the millimeter-wave region. For those states, only partial fits are reported. Concerning the energy order of ν_{42} and ν_{23}, which is an important starting point to treat the perturbation involving these two states, we assume that ν_{42} is the lowest excited state in energy as weak transitions of ν_{42} were observed by jet-cooled rotational spectroscopy in the 2-8 GHz range.

This work across multiple spectral ranges led to a better characterization of all the skeletal ring modes of THP and an accurate determination of the vibrational frequencies of these motions. This shows how complementary data obtained with different techniques probing various frequency regions and investigating distinct molecular motions can be combined to result in a broader dataset which describes the properties of a molecule with a significantly improved accuracy. Furthermore, learning about the pyranose ring will give insight into further investigations on more complex molecules such as carbohydrates. With the recent developments in radio astronomy, more and more complex molecules are being identified in places like the interstellar medium.[33,34] Many of these molecules have biological relevance and are important in the ongoing quest to answer the question about the origin of life. For a successful detection, accurate laboratory molecular parameters are required for both ground and vibrationally excited states, such as those provided in the present work for THP. Since THP resembles the backbone of a sugar, its successful observation might be an important puzzle piece to reveal biochemical processes in space.

Conflicts of interest

"There are no conflicts to declare".

Acknowledgements

The authors thank the AILES beamline staff at the synchrotron SOLEIL for technical support during the beamtime. A.L.S. thanks "The Hamburg Centre for Ultrafast Imaging" for funding via a Louise Johnson fellowship. This work was supported by the ERC Starting Grant "ASTROROT", grant number 638027.

Notes and references

1 E. Cocinero, E. Stanca-Kaposta, M. Dethlefsen, B. Liu, D. Gamblin, B. Davis and J. Simons, *Chemistry – A European Journal*, 2009, **15**, 13427–13434.

2 F. Gámez, B. Martínez-Haya, S. Blanco, J. C. López and J. L. Alonso, *The Journal of Physical Chemistry Letters*, 2012, **3**, 482–485.

3 V. A. Shubert, W. H. James and T. S. Zwier, *The Journal of Physical Chemistry A*, 2009, **113**, 8055–8066.

4 C. Pérez, J. C. López, S. Blanco and M. Schnell, *The Journal of Physical Chemistry Letters*, 2016, **7**, 4053–4058.

5 J. A. Greenhouse and H. L. Strauss, *The Journal of Chemical Physics*, 1969, **50**, 124–134.

6 M. Winnewisser, M. Kunzmann, M. Lock and B. P. Winnewisser, *Journal of Molecular Structure*, 2001, **561**, 1–15.

7 V. M. Rao and R. Kewley, *Canadian Journal of Chemistry*, 1969, **47**, 1289–1293.

8 R. S. Lowe and R. Kewley, *Journal of Molecular Spectroscopy*, 1976, **60**, 312–323.

9 U. Spoerel, W. Stahl, W. Caminati and P. G. Favero, *Chemistry – A European Journal*, 1998, **4**, 1974–1981.

10 D. Vedal, O. H. Ellestad, P. Klaboe and G. Hagen, *Spectrochimica Acta Part A: Molecular Spectroscopy*, 1975, **31**, 339–354.

11 J. C. Lopez, J. L. Alonso and R. M. Villamañan, *Journal of Molecular Structure*, 1986, **147**, 67–76.

12 G. G. Brown, B. C. Dian, K. O. Douglass, S. M. Geyer, S. T. Shipman and B. H. Pate, *Review of Scientific Instruments*, 2008, **79**, 053103.

13 C. Pérez, S. Lobsiger, N. A. Seifert, D. P. Zaleski, B. Temelso, G. C. Shields, Z. Kisiel and B. H. Pate, *Chemical Physics Letters*, 2013, **571**, 1–15.

14 D. Schmitz, V. Alvin Shubert, T. Betz and M. Schnell, *Journal of Molecular Spectroscopy*, 2012, **280**, 77–84.

15 C. Pérez, A. Krin, A. L. Steber, J. C. López, Z. Kisiel and M. Schnell, *The Journal of Physical Chemistry Letters*, 2016, **7**, 154–160.

16 J. L. Neill, B. J. Harris, A. L. Steber, K. O. Douglass, D. F. Plusquellic and B. H. Pate, *Optics Express*, 2013, **21**, 19743–19749.

17 B. E. Arenas, S. Gruet, A. L. Steber, B. M. Giuliano and M. Schnell, *Physical Chemistry Chemical Physics*, 2017, **19**, 1751–1756.

18 B. E. Arenas, S. Gruet, A. L. Steber and M. Schnell, *Journal of Molecular Spectroscopy*, 2017, **337**, 9–16.

19 J.-B. Brubach, L. Manceron, M. Rouzières, O. Pirali, D. Balcon, F. K. Tchana, V. Boudon, M. Tudorie, T. Huet, A. Cuisset and P. Roy, *AIP Conference Proceedings*, 2010.

20 F. Freeman, M. L. Kasner and W. J. Hehre, *The Journal of Physical Chemistry A*, 2001, **105**, 10123–10132.

21 Z. Kisiel, L. Pszczółkowski, I. R. Medvedev, M. Winnewisser, F. C. De Lucia and E. Herbst, *Journal of Molecular Spectroscopy*, 2005, **233**, 231–243.

22 W. Łodyga, M. Kreglewski, P. Pracna and Š. Urban, *Journal of Molecular Spectroscopy*, 2007, **243**, 182–188.

23 M. J. Frisch, G. W. Trucks, H. B. Schlegel, G. E. Scuseria, M. A. Robb, J. R. Cheeseman, G. Scalmani, V. Barone, B. Mennucci, G. A. Petersson, H. Nakatsuji, M. Caricato, X. Li, H. P. Hratchian, A. F. Izmaylov, J. Bloino, G. Zheng, J. L. Sonnenberg, M. Hada, M. Ehara, K. Toyota, R. Fukuda, J. Hasegawa, M. Ishida, T. Nakajima, Y. Honda, O. Kitao, H. Nakai, T. Vreven, J. A. Montgomery, Jr., J. E. Peralta, F. Ogliaro, M. Bearpark, J. J. Heyd, E. Brothers, K. N. Kudin, V. N. Staroverov, R. Kobayashi, J. Normand, K. Raghavachari, A. Rendell, J. C. Burant, S. S. Iyengar, J. Tomasi, M. Cossi, N. Rega, J. M. Millam, M. Klene, J. E. Knox, J. B. Cross, V. Bakken, C. Adamo, J. Jaramillo, R. Gomperts, R. E. Stratmann, O. Yazyev, A. J. Austin, R. Cammi, C. Pomelli, J. W.

Ochterski, R. L. Martin, K. Morokuma, V. G. Zakrzewski, G. A. Voth, P. Salvador, J. J. Dannenberg, S. Dapprich, A. D. Daniels, Ã. Farkas, J. B. Foresman, J. V. Ortiz, J. Cioslowski and D. J. Fox, *Gaussian 09 Revision D.01*, Gaussian Inc. Wallingford CT 2009.

24 H. M. Pickett, *Journal of Molecular Spectroscopy*, 1991, **148**, 371–377.

25 J. Kraitchman, *American Journal of Physics*, 1953, **21**, 17–24.

26 Z. Kisiel, *Spectroscopy from Space*, Springer, Dordrecht, 2001, pp. 91–106.

27 J. Dommen, T. Brupbacher, G. Grassi and A. Bauder, *Journal of the American Chemical Society*, 1990, **112**, 953–957.

28 G. Gundersen and D. Rankin, *Acta Chemica Scandinavica Series a-Physical and Inorganic Chemistry*, 1983, **37**, 865–874.

29 M. Fargher, L. Hedberg and K. Hedberg, *Journal of Molecular Structure*, 2014, **1071**, 41–44.

30 F. Matsushima, H. Odashima, T. Iwasaki, S. Tsunekawa and K. Takagi, *Journal of Molecular Structure*, 1995, **352**, 371–378.

31 V. M. Horneman, R. Anttila, S. Alanko and J. Pietilä, *Journal of Molecular Spectroscopy*, 2005, **234**, 238–254.

32 O. Pirali, Z. Kisiel, M. Goubet, S. Gruet, M. A. Martin-Drumel, A. Cuisset, F. Hindle and G. Mouret, *The Journal of Chemical Physics*, 2015, **142**, 104310.

33 A. Belloche, R. T. Garrod, H. S. P. Müller and K. M. Menten, *Science*, 2014, **345**, 1584–1587.

34 B. A. McGuire, A. M. Burkhardt, S. Kalenskii, C. N. Shingledecker, A. J. Remijan, E. Herbst and M. C. McCarthy, *Science*, 2018, **359**, 202–205.